A Hierarchical Harmonic Control Method for Wind Power Plants in Microgrids

Li, Shuting; Wu, Jingxuan; Tinajero, Gibran David Agundis; Chaudhary, Sanjay K.; Vasquez, Juan C.; Guerrero, Josep M.

Published in:
IECON 2023 - 49th Annual Conference of the IEEE Industrial Electronics Society

DOI (link to publication from Publisher):
10.1109/IECON51785.2023.10312706

Publication date:
2023

Document Version
Accepted author manuscript, peer reviewed version

A Hierarchical Harmonic Control Method for Wind Power Plants in Microgrids

Shuting Li[a], Jingxuan Wu[a], Gibran D. Agundis-Tinajero[a], Sanjay Chaudhary[a]
Juan C. Vasquez[a], Josep M. Guerrero[a]
[a] Department of AAU Energy, Aalborg University, Aalborg, Denmark
{shuli, jinwu, gdat, skc, juq, joz}@energy.aau.dk

***Abstract*—For multibus wind power plants in microgrids, it is challenging to develop a reliable, effective, and robust harmonic suppression method for harmonic voltages and currents of all buses. This paper proposes a hierarchical harmonic control method to mitigate the harmonic voltages and currents of all buses in grid-forming wind power plants. The proposed method effectively reduces the terminal harmonic voltages and currents, PCC harmonic voltage, and grid harmonic current. It achieves adaptive harmonic mitigation and automatic harmonic current sharing between wind turbine units according to the rated capacity and feeder impedance of each unit. The effectiveness of the method is verified in the planned Turkish offshore wind power plant by simulation in Digsilent/PowerFactory.**

***Index Terms*—harmonic mitigation, harmonic current sharing, microgrids, wind power plant**

I. Introduction

Microgrids offer an effective approach to incorporating renewable energy resources, such as wind, photovoltaic, etc., into distribution systems by constructing a hierarchical infrastructure [1]. Grid compliance of microgrids concerning harmonics presents unique challenges to the hierarchical control architecture of microgrids. On the one hand, due to the proliferation of power electronic equipment, including wind turbines (WT) and power converters, wind power plants (WPP) have increased the harmonic emissions in microgrids [2], which affects the reliability of WPPs as power sources for microgrids. On the other hand, wind-power-integrated microgrids are always located in remote areas, where the grid is easily distorted by the increased penetration of nonlinear loads. This part of the harmonics of the grid is called grid background harmonic voltage. The background harmonics further increase the uncertainty and the harmonic distortion of the generated wind power, which will cause malfunction or overheating of devices or motors. Improving the power quality of WPPs in microgrids is, therefore, of significant importance.

The main strategies to enhance power quality in wind-power-integrated microgrids are as follows: (1) harmonic voltage mitigation at points of common coupling (PCCs); (2) grid harmonic current suppression; and (3) wind turbine output harmonic current cancellation. Most harmonic mitigation methods are proposed in the primary control layer to achieve one or more of the above objectives for single converter-based systems. These methods are implemented at the primary control layer along with common controllers, such as droop controllers or virtual synchronous generator (VSG) controllers, to mitigate harmonic distortion. For grid-connected converters, the virtual impedance methods [2]–[5], which act as feedback-only approaches, give flexible harmonic voltage reduction for a voltage-controlled converter by adopting appropriate converter output currents or grid current as feedback references. The virtual admittance methods are another kind of feedback-only methods, which obtain flexible harmonic current mitigation for a current-controlled converter [6] [7]. These feedback-only methods may result in system instability problems due to high dependence of the overlarge feedback gains. The feedforward PCC voltage methods reduce the harmonics for voltage-controlled converters by adopting PCC voltages as feedforward references [8], not influencing the pole-zero distribution of the system but still have the possibility of overmodulation problem due to the overlarge feedforward gains. The hybrid impedance-based methods [9] [10] reduce the reliability of over-increasing feedback or feedforward gains, but are still sensitive to system parameters such as converter rated capacity, feeder impedance, and distribution of wind turbine units. This greatly affects the robustness of harmonic control for microgrids. In addition, the mitigation of voltage and current harmonics of all buses needs more attention in the multibus system, especially in networked microgrids with dynamic boundary, which dynamically includes or excludes part of utility networks for various operation purposes [3]. These multibus systems pose additional challenges for harmonic mitigation due to their complex architecture and control objectives.

For the secondary control layer of WPP in microgrids, two control schemes are mainly used for harmonic mitigation. One is centralized control, and the other is distributed control. The former uses online information from wind turbine units to make the harmonic control decision and send the control signal to the local controllers. The latter, more commonly applied in grid-connected systems with multi-wind-turbine units, collects all information and makes control decisions at the local harmonic controllers. The virtual admittance methods [11] [12] can also be implemented at the secondary control layer for their low complexity. Some harmonic extraction and compensation methods [13] [14], such as second-order

This work is supported in part by China Scholarship Council (CSC) and in part by the Offshore Wind Farms Large-scale Integration in Turkey (WindFlag) project (Project No. 19-M03-AAU), which is sponsored by the Ministry of Foreign Affairs of Denmark and supported by Danida Fellowship Centre.

generalized integrators (SOGI), reduced-order generalized integrators (ROGI), proportional resonance (PR) controllers, etc., which is similar with primary layer, are also implemented at this level to send harmonic component references to primary level. The consensus protocol-based distributed controller is also proposed at the secondary layer to adaptively regulate the virtual impedance for power quality improvement and harmonic current sharing [15]. These harmonic mitigation methods used at the secondary control layer reduce the sensitivity to system parameters compared to methods implemented at the primary control layer. However, harmonic voltages and current mitigation of multiple buses still need to be considered. In addition, the adaptive or predictive approach can be used at this level to improve harmonic control adaptivity.

Based on the above analysis, it is vital to propose a reliable, effective, and robust harmonic suppression method for both harmonic voltages and currents at PCCs and all buses of WPPs in microgrids. Note that this paper only focuses on the harmonic suppression in the WPP part which feeds the microgrid. The way to compensate for the local nonlinear load harmonics of the microgrid is out of scope. In this paper, a hierarchical harmonic control architecture for multibus WPPs in microgrids is proposed. The PCC harmonic voltages and grid currents are mitigated. The harmonic distortion mitigation of all buses and terminals is performed. A droop-based harmonic current sharing strategy further reduces the harmonic control sensitivity. The rest of the paper is organized as follows: Section II gives the hierarchical harmonic control architecture. The primary harmonic control strategy, secondary harmonic control strategy, and droop-based harmonic current sharing strategy are also discussed in this section. Then the simulation results of harmonic suppression performance and harmonic current sharing performance are given in Section III. Finally, conclusions are drawn in Section IV.

II. Hierarchical Harmonic Control Architecture

For the WPP in microgrids, hierarchical control is used to improve reliability and efficiency in the operation of the system. It is worth noting that the following discussion regarding the WPP is based on a planned offshore wind power plant (OWPP) in Turkey, and the harmonic analysis is also based on a single converter unit for simplicity.

A. Overall Harmonic Control Architecture

Fig. 1 shows the architecture and basic voltage and frequency control strategy of the WPP in microgrids based on the Turkish OWPP. In Fig. 1(a), 60 wind turbine generators (WTGs) (6 WTGs per feeder) are connected to a common bus. The wind power generated by the wind turbine part feeds the substation grid at the PCC. In Fig. 1(b), the rotor-side converters of wind turbines are controlled by the maximum power point tracking (MPPT) algorithm. The grid-side converters are controlled by the grid-forming VSG controller proposed in [16]. Fig. 2 shows the overall harmonic control strategy for the WPP, which is implemented on the grid-side converters of wind turbines. The wind turbine output current i_o, capacitor voltage v_c, terminal current i_t, PCC voltage v_{pcc}, and grid current i_g are measured as shown in Fig. 2. The harmonic compensation signal generated by the harmonic controller is added to the VSG control output signal and injected into the PWM modulator to reduce the harmonic component of all buses.

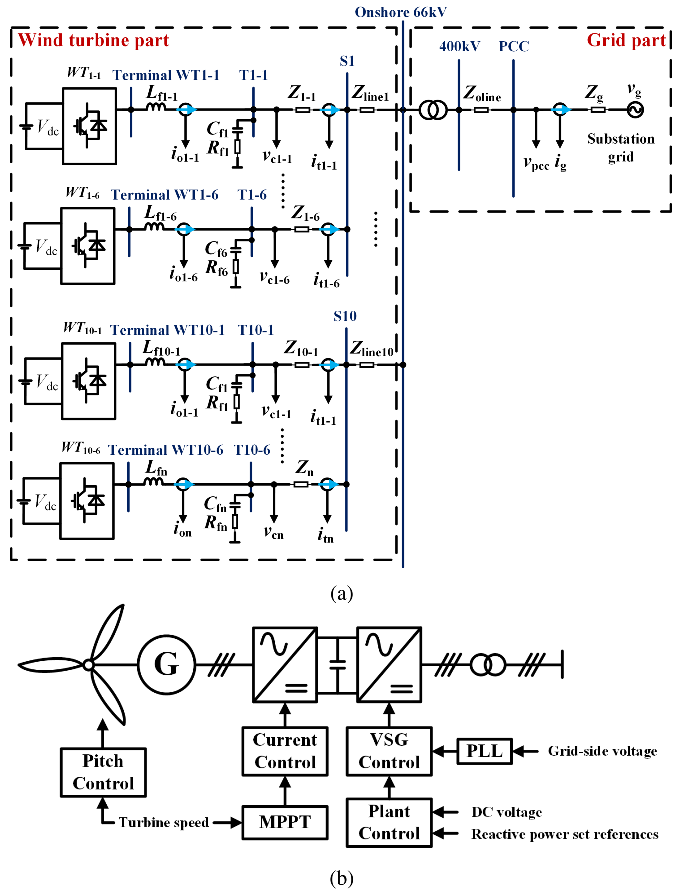

Fig. 1. Electrical and control part of the WPP in microgrids. (a) Electrical part. (b) Control part.

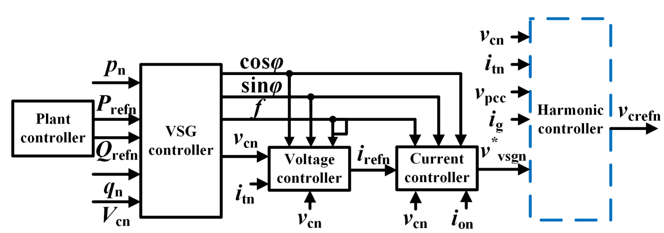

Fig. 2. Overall harmonic control strategy.

B. Harmonic Primary Control

On the harmonic primary control layer, the control objective is to mitigate the harmonic distortion of terminal voltages and currents in the wind turbine part and share the harmonic currents among the converters. The harmonics of the current i_{tn} in Fig. 1(a) result from the converters and grid background harmonics. In this sense, a hybrid impedance-based (HI) harmonic mitigation strategy is applied to reduce the terminal voltage and current harmonics. The VSG output voltage v_{cn} and the current i_{tn} are extracted to form the primary harmonic control (PHC) loop in Fig. 3(a). The factor x is a feedforward coefficient for capacitor voltage v_{cn}, and the factor Z_v can be regarded as a virtual impedance. The signal e_{refn} is the VSG control output voltage. The factors x and Z_v can be coordinated to effectively reduce the terminal harmonic distortion. Fig. 3(b) shows the equivalent harmonic model of the wind turbine part with the HI harmonic control strategy. The WT converter controlled by PHC is equivalent to a harmonic voltage source V_{vsgh} in series with two controlled voltage sources and an output impedance Z_{on}. The background harmonic voltage of the terminal is represented by an equivalent harmonic voltage source V_{th}. The capacitor Z_s is the shunt-connected capacitance. The impedance Z_o in Fig. 3(b) is the sum of the VSG output impedance Z_{on} and the filter impedance Z_{fn}.The subscript h means the harmonic component of each variable. From Fig. 3(b), the harmonic current I_{th} flowing through the terminal is controlled as

$$I_{th} = \frac{Z_s V_{vsgh} - [(1-x)Z_s + Z_o]V_{th}}{(Z_s Z_o + (1-x)Z_s Z_n + Z_v Z_s + Z_o Z_n)} \quad (1)$$

The total impedance viewed from the terminal to the converter is consequently reshaped as

$$Z_{TC} = \frac{Z_o Z_s + Z_v G_h(s) Z_s + [1 - xG_h(s)]Z_s Z_n + Z_o Z_n}{[1 - xG_h(s)]Z_s + Z_o} \quad (2)$$

Where the G_h represents the reduced order generalized integrators (ROGIs) [17] to extract v_{cn} and i_{tn}. The G_h is expressed as

$$G_h = \sum_{h=-5,7,-11,13,-17,19} \frac{K_r \omega_c}{s - jh\omega_n + \omega_c} \quad (3)$$

Where ω_n is the fundamental frequency of the grid-side converter and ω_c is the cut-off frequency of band-pass filters. The magnitude of the filter is increased to 0dB at positive 7th, 13th, 19th frequencies and negative -5th, -11th, -17th frequencies to effectively extract the harmonic components at these harmonic frequencies.

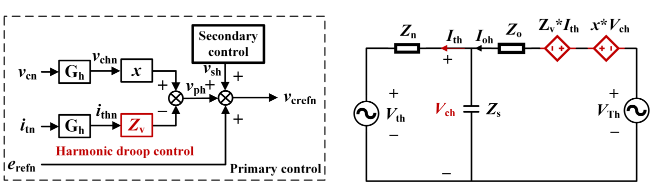

(a) (b)

Fig. 3. Primary harmonic controller of wind turbine part. (a) PHC strategy. (b) The equivalent harmonic model with PHC

With proper design of factor x and virtual impedance Z_v, the harmonic component I_{th}/V_{vsgh} and I_{th}/V_{th} can be effectively reduced, and the total harmonic impedance of the wind turbine part is increased at main harmonic frequencies, which mean the terminal harmonic current and voltage can be effectively reduced through PHC.

C. Harmonic Secondary Control

The harmonic secondary control further suppresses the harmonics at PCCs caused by converters and grid background harmonics. The hybrid harmonic control strategy is also applied to the secondary control layer. The PCC voltage v_{pcc} and grid current i_g are extracted to form a secondary harmonic control (SHC) loop, as shown in Fig. 4(a). The filter G_h extracts the fundamental components of v_{pcc} and i_g. The following analysis is focused on the grid harmonic current reduction. While the control strategy is effective for both PCC harmonic voltage mitigation and grid harmonic current reduction in this case. The equivalent harmonic model of the grid part with HI strategy is obtained in Fig. 4(b). The wind turbine part is equivalent to a harmonic voltage source V_{Th} in series with an impedance Z_{Tn}. The grid background harmonic voltage is equivalent to a harmonic voltage source V_{gh}. Z_T is the sum of the Z_{Tn} and line impedance Z_{line}. From the equivalent model, the grid harmonic current and the PCC harmonic voltage can be obtained as

$$I_{gh} = \frac{Z_s V_{Th} - [(1-x)Z_s + Z_T] * V_{gh}}{(Z_s Z_T + (1-x)Z_s Z_g + Z_v s Z_s + Z_T Z_g)} \quad (4)$$

The total impedance viewed from the grid to the terminal is therefore controlled as

$$Z_{GT} = \frac{Z_T Z_s + Z_v s G_h(s) Z_s + [1 - xG_h(s)]Z_s Z_g + Z_T Z_g}{[1 - xG_h(s)]Z_s + Z_T} \quad (5)$$

With proper design of the factor x_s and Z_{vs}, the total impedance viewed from the grid to the terminal can be increased to reduce the harmonic components I_{gh}/V_{Th} and I_{gh}/V_{gh} by SHC.

Finally, the modified voltage reference of each converter with the hierarchical harmonic controller can be obtained as

$$v_{crefn} = v^*_{vsgn} + xv_{Thn} - Z_v i_{Thn} + x_s v_{pcch} - Z_{vs} i_{gh} \quad (6)$$

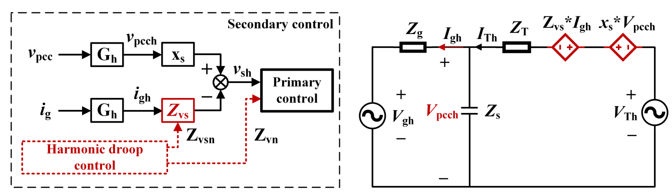

(a) (b)

Fig. 4. Secondary harmonic controller of grid part. (a) SHC strategy. (b) The equivalent harmonic model with SHC

D. Droop-based Harmonic Current Sharing Strategy Design

Based on the above discussion, the harmonic current or harmonic voltage mitigation depends on the total impedance. Taking the primary control as an example, the harmonic suppression performance is decided by the factor Z_v When factor x is fixed. It is worth noting that the factor Z_v should not be too large to cause the system instability problem. On the other hand, the harmonic current should be shared among converters properly based on their different rated capacities and feeder impedances. In this sense, a droop-based harmonic current sharing strategy is proposed to define the harmonic compensation factor. In this paper, the virtual impedance Z_v can be set as sL_v for simplicity. The droop-based characteristic is given as

$$L_v = L^* + D_H(H_r + H) \tag{7}$$

Where L^* is the reference value of L_v. The D_H is the droop coefficient to automatically control the harmonic mitigation factor. The H_r is the converter's available capacity for harmonic suppression, which can be calculated as

$$H_r = \sqrt{S_{rated}^2 - P_f^2 - Q_f^2} \tag{8}$$

Where S_{rated} is the rated capacity of each converter. The P_f and Q_f are the converter's fundamental active power and reactive power, respectively. The H is the distortion power of the converter, which can be calculated as [8]

$$H = \sqrt{S_{actual}^2 - P_f^2 - Q_f^2} \tag{9}$$

Where S_{actual} is the converter's actual output apparent power, which can be obtained as $V_{cRMS} * I_{oRMS}$.

The background harmonics are not constant for large WPPs connected to the substation grid. When the background harmonics increase, the converter output harmonic power H will increase accordingly. Then the harmonic control factor L_v will be increased by the droop-based harmonic current sharing controller to increase the equivalent output impedance of the converter and consequently reduce the converter output harmonic current. Furthermore, when the converters are distributed equally with the same rated capacity, each converter's harmonic control factor L_v of each converter will be equal. When the feeder impedance of WT1 is smaller than the feeder impedance of WT2, the WT1 harmonic output power H_1 will be larger than the WT2 harmonic output power H_2. With the droop-based harmonic current sharing strategy, the WT1 harmonic compensation factor L_{v1} is controlled to be larger than the WT2 factor L_{v2}. Then the WT1 total impedance Z_{TC1} becomes larger than WT2 total impedance Z_{TC2}. Consequently, the harmonic output current I_{th1} decreases to be equal to I_{th1} and H_1 decreases to be equal to H_2. In (7), the output value of the factor L_v is also proportional to the converter's available capacity. The L_v can be reduced with the converter available capacity H_r decreasing to avoid system instability. This droop-based harmonic current sharing strategy realizes adaptive harmonic mitigation and automatic harmonic sharing between WT units.

III. Simulation of Proposed Method in Turkish OWPP

The hierarchical harmonic control architecture is evaluated in the planned Turkish OWPP by simulation using the software DigSilent/PowerFactory (version 2022 SP1). The harmonic primary and secondary controllers are implemented in the $\alpha\beta$ axis. The parameters of the harmonic controller are given in Table I. In this case, the compensation factor L_{vs} of the secondary controller can be set to 0. The harmonics of wind turbines and background harmonics in the simulation are simulated as Fourier series added on the capacitor voltage v_{cn} and the PCC voltage v_{pcc} in the control model.

TABLE I
Harmonic Controller Parameters

	Symbol	Parameter	Value
Band pass filter	K_r	Gain	1
	ω_n	Fundamental frequency	100π
	ω_c	Cut-off frequency	5
Primary controller	x	Feedforward factor	1
Secondary controller	x_s	Feedforward factor	1
	L^*	Reference factor	0.03
	D_H	Droop coefficient	0.01

A. Harmonic Suppression Performance Analysis

The harmonic suppression performance of the proposed method is validated in Fig. 5 - Fig. 7. The hierarchical harmonic control is removed at 12s. In Fig. 5, the PCC voltage and grid current are presented. Comparing Fig. 5(a) and (b), the total harmonic distortion (THD) of the PCC voltage is reduced from 3.09% to 1.36% with the hierarchical harmonic control. And the THD of the grid current is reduced from 3.12% to 1.52%. The PCC voltage distortion and the grid current distortion are effectively reduced. Fig. 6 shows the harmonic voltage mitigation results of onshore terminals. Compared to Fig. 6(b), the total harmonic distortion of the onshore 66kV terminal voltage is reduced from 3.93% to 1.81% with the hierarchical harmonic control in Fig. 6(a). And the THD of the onshore 400kV terminal voltage is reduced from 3.44% to 1.53%. Fig. 7 shows the voltage and current results of WT terminals. The THD of the Terminal 1-1 voltage is reduced from 3.77% to 1.81% with the hierarchical harmonic control. And the THD of the current flows from WT 1-1 is reduced from 5.29% to 2.19%. The THD of the current flows from Terminal 1-1 is reduced from 3.25% to 1.14%. Fig. 5 - Fig. 7 validate the effectiveness of the proposed harmonic control method for multibus wind-power-integrated microgrids.

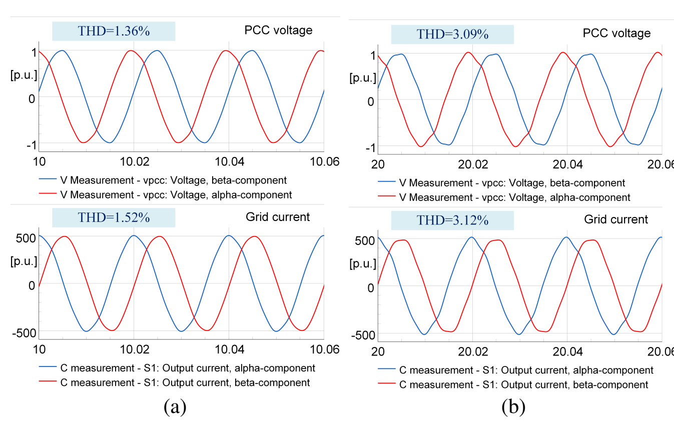

Fig. 5. Harmonic suppression performance results of PCC. (a) With proposed HHC. (b) Without HHC.

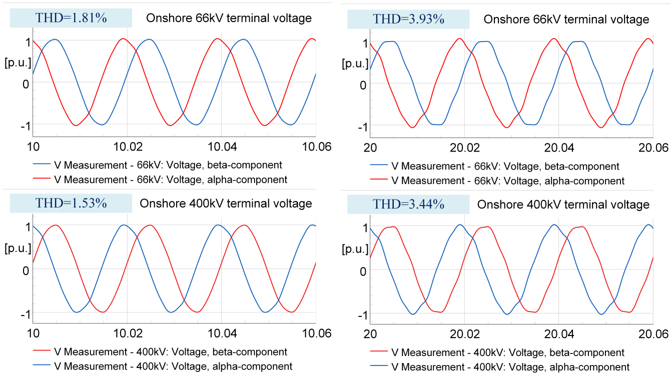

(a) (b)

Fig. 6. Harmonic suppression performance results of onshore terminals. (a) With proposed HHC. (b) Without HHC.

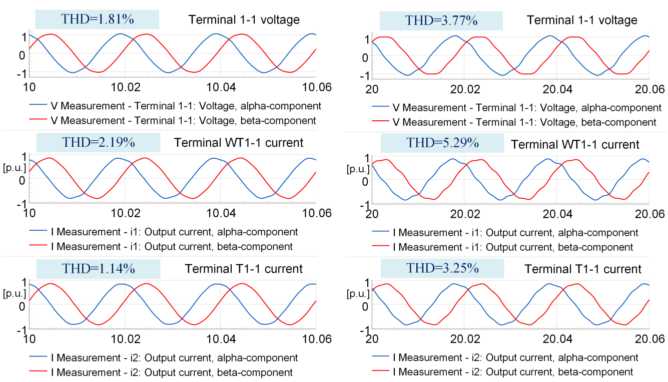

(a) (b)

Fig. 7. Harmonic suppression performance results of WT terminals. (a) With proposed HHC. (b) Without HHC.

B. Harmonic Current Sharing Performance Analysis

Based on the Turkish OWPP, the potential capacity analysis assumed the same wind distribution in all cases. In this sense, the harmonic current sharing performance is only verified in scenarios with equal ratings, but different PCC set powers. Fig. 8 and Fig. 9 give the comparative simulation results with the fixed harmonic factor Z_v and droop-based factor Z_v. To avoid the mutation, the PCC set power ramps up from 0.85 pu to 0.92 pu at 12s in Fig. 8 and Fig. 9. The Z_v value ramps up to the fixed value in Fig. 9 at the beginning of the simulation. In Fig. 8, the system power oscillates when the PCC power is close to the rated value with the fixed harmonic mitigation factor Z_v. However, the harmonic control still performs well with the droop-based harmonic current sharing strategy in Fig. 9.

IV. Conclusion

In this paper, a hierarchical harmonic control architecture is proposed for multibus WPP in microgrids. The harmonic primary controller mitigates the terminal harmonic voltages and currents of the wind turbine part. The harmonic secondary controller reduces the harmonic distortion of the PCC voltage and grid current. A droop-based harmonic current sharing controller is further developed on the secondary control layer to improve the harmonic flexibility and solve the harmonic current sharing problem between WT units.

The proposed method is verified in a planned Turkish OWPP by simulation in DigSilent/PowerFactory. According to the simulation results, the proposed method effectively mitigates the harmonic distortion of WT terminal voltages, onshore terminal voltages, PCC voltage, and grid current. The proposed method is further verified in scenarios with equal WT distribution and different PCC set powers. The system power oscillates when the PCC power is closed to the rated value with the fixed harmonic mitigation factor Z_v. However, the harmonic control performs well with the droop-based harmonic current sharing strategy. The harmonic control flexibility is improved. And the harmonic power is shared appropriately among WT units according to their rated capacities and feeder impedances.

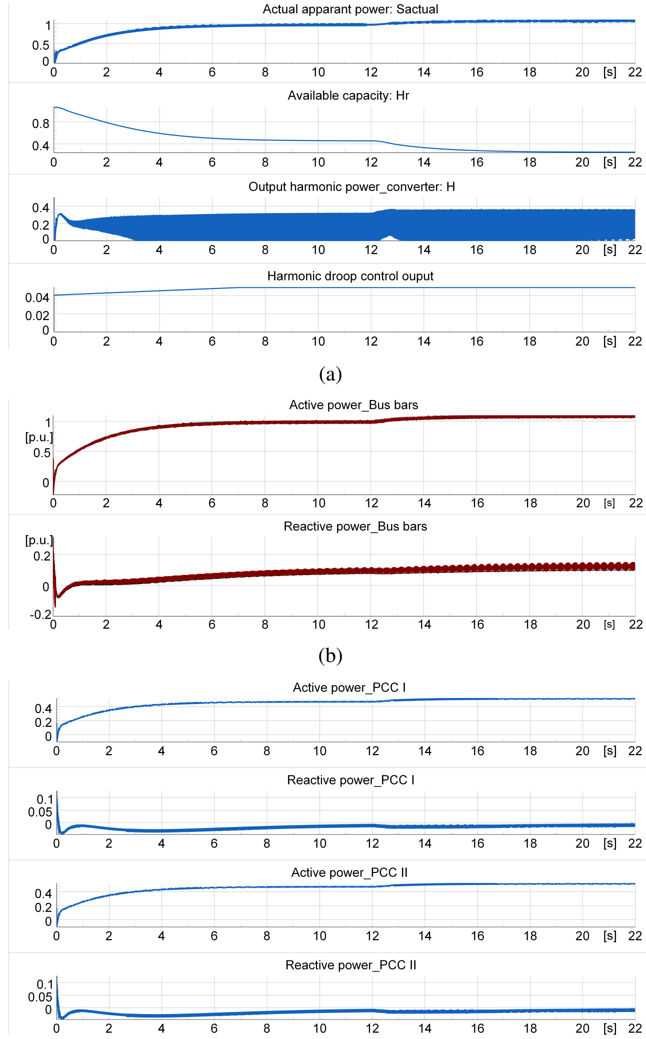

(c)

Fig. 8. Harmonic current sharing results with fixed harmonic control factor and different set power.

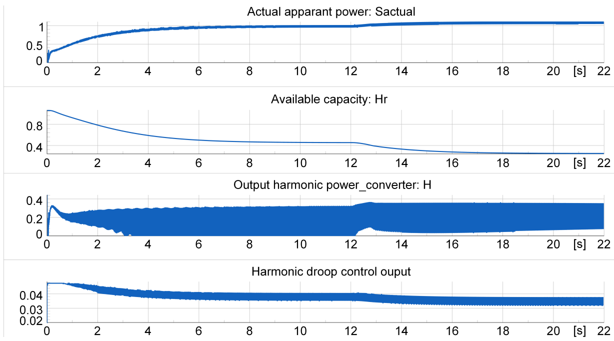

(a)

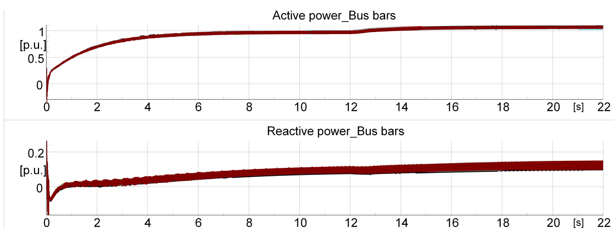

(b)

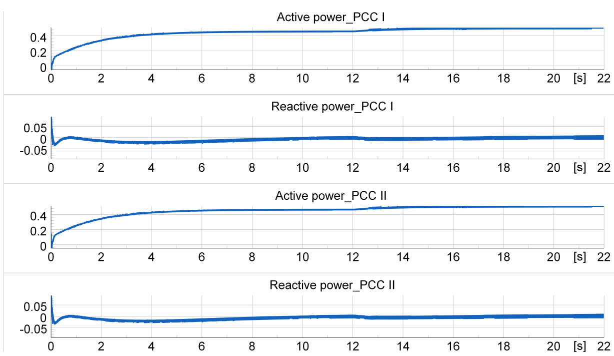

(c)

Fig. 9. Harmonic current sharing results with droop-based harmonic current sharing control and different set power.

References

[1] B. Chen, J. Wang, X. Lu, C. Chen, and S. Zhao, "Networked Microgrids for Grid Resilience, Robustness, and Efficiency: A Review," *IEEE Transactions on Smart Grid*, vol. 12, no. 1, pp. 18–32, Jan. 2021, conference Name: IEEE Transactions on Smart Grid.

[2] E. Guest, K. H. Jensen, and T. W. Rasmussen, "Mitigation of Harmonic Voltage Amplification in Offshore Wind Power Plants by Wind Turbines With Embedded Active Filters," *IEEE Transactions on Sustainable Energy*, vol. 11, no. 2, pp. 785–794, Apr. 2020, conference Name: IEEE Transactions on Sustainable Energy.

[3] Y. Han, P. Shen, X. Zhao, and J. M. Guerrero, "Control Strategies for Islanded Microgrid Using Enhanced Hierarchical Control Structure With Multiple Current-Loop Damping Schemes," *IEEE Transactions on Smart Grid*, vol. 8, no. 3, pp. 1139–1153, May 2017.

[4] S. Y. Mousazadeh Mousavi, A. Jalilian, M. Savaghebi, and J. M. Guerrero, "Autonomous Control of Current- and Voltage-Controlled DG Interface Inverters for Reactive Power Sharing and Harmonics Compensation in Islanded Microgrids," *IEEE Transactions on Power Electronics*, vol. 33, no. 11, pp. 9375–9386, Nov. 2018, conference Name: IEEE Transactions on Power Electronics.

[5] F. Deng, X. Li, X. Zhang, and P. Mattavelli, "An Iterative Virtual Impedance Regulation Strategy in Islanded Microgrids for Enhanced Balanced, Unbalanced and Harmonic Current Sharing," *IEEE Transactions on Sustainable Energy*, vol. 13, no. 1, pp. 514–526, Jan. 2022.

[6] A. Micallef, M. Apap, C. Spiteri-Staines, and J. M. Guerrero, "Mitigation of Harmonics in Grid-Connected and Islanded Microgrids Via Virtual Admittances and Impedances," *IEEE Transactions on Smart Grid*, vol. 8, no. 2, pp. 651–661, Mar. 2017, conference Name: IEEE Transactions on Smart Grid.

[7] Q. Qian, S. Xie, J. Xu, S. Bian, and N. Zhong, "Passivity-based output admittance shaping of the converter-side current-controlled grid-tied inverter to improve the robustness to the grid impedance," *IET Power Electronics*, vol. 13, no. 10, pp. 1956–1965, 2020.

[8] P. Sreekumar and V. Khadkikar, "Direct Control of the Inverter Impedance to Achieve Controllable Harmonic Sharing in the Islanded Microgrid," *IEEE Transactions on Industrial Electronics*, vol. 64, no. 1, pp. 827–837, Jan. 2017.

[9] J. He, Y. W. Li, and F. Blaabjerg, "Flexible Microgrid Power Quality Enhancement Using Adaptive Hybrid Voltage and Current Controller," *IEEE Transactions on Industrial Electronics*, vol. 61, no. 6, pp. 2784–2794, Jun. 2014.

[10] L. Zhou, Z. Shuai, Y. Chen, W. Wu, X. Zhou, K. Yan, and A. Luo, "Impedance-Based Harmonic Current Suppression Method for VSG Connected to Distorted Grid," *IEEE Transactions on Industrial Electronics*, vol. 67, no. 7, pp. 5490–5502, Jul. 2020.

[11] C. Blanco, D. Reigosa, J. C. Vasquez, J. M. Guerrero, and F. Briz, "Virtual Admittance Loop for Voltage Harmonic Compensation in Microgrids," *IEEE Transactions on Industry Applications*, vol. 52, no. 4, pp. 3348–3356, Jul. 2016, conference Name: IEEE Transactions on Industry Applications.

[12] C. Blanco, F. Tardelli, D. Reigosa, P. Zanchetta, and F. Briz, "Design of a Cooperative Voltage Harmonic Compensation Strategy for Islanded Microgrids Combining Virtual Admittance and Repetitive Controller," *IEEE Transactions on Industry Applications*, vol. 55, no. 1, pp. 680–688, Jan. 2019, conference Name: IEEE Transactions on Industry Applications.

[13] M. Savaghebi, J. M. Guerrero, A. Jalilian, and J. C. Vasquez, "Mitigation of voltage and current harmonics in grid-connected microgrids," in *2012 IEEE International Symposium on Industrial Electronics*, May 2012, pp. 1610–1615, iSSN: 2163-5145.

[14] M. S. Golsorkhi, M. Savaghebi, D. D.-C. Lu, J. M. Guerrero, and J. C. Vasquez, "A GPS-Based Control Framework for Accurate Current Sharing and Power Quality Improvement in Microgrids," *IEEE Transactions on Power Electronics*, vol. 32, no. 7, pp. 5675–5687, Jul. 2017, conference Name: IEEE Transactions on Power Electronics.

[15] J. Zhou, S. Kim, H. Zhang, Q. Sun, and R. Han, "Consensus-Based Distributed Control for Accurate Reactive, Harmonic, and Imbalance Power Sharing in Microgrids," *IEEE Transactions on Smart Grid*, vol. 9, no. 4, pp. 2453–2467, Jul. 2018, conference Name: IEEE Transactions on Smart Grid.

[16] Y. Yu, S. K. Chaudhary, G. D. A. Tinajero, L. Xu, N. N. B. A. Bakar, J. C. Vasquez, and J. M. Guerrero, "A Reference-Feedforward-Based Damping Method for Virtual Synchronous Generator Control," *IEEE Transactions on Power Electronics*, vol. 37, no. 7, pp. 7566–7571, Jul. 2022.

[17] C. Xie, X. Zhao, K. Ki, D. Liu, J. M. Guerrero, and J. C. Vasquez, "Phase Compensated Reduced Order Generalized Integrators for Grid-Tied VSCs With Harmonics Compensation Capability," *IEEE Transactions on Industry Applications*, vol. 54, no. 3, pp. 2568–2578, May 2018.